

Development of an engineering material with increased impact strength and heat
resistance from recycled PET

Slezák E., Ronkay F., Bocz K.

Accepted for publication in Journal of Polymers and the Environment

Published in 2023

DOI: [10.1007/s10924-023-02945-4](https://doi.org/10.1007/s10924-023-02945-4)



Development of an Engineering Material with Increased Impact Strength and Heat Resistance from Recycled PET

Emese Slezák¹ · Ferenc Ronkay² · Katalin Bocz¹

Accepted: 31 May 2023 / Published online: 30 June 2023
© The Author(s) 2023

Abstract

The goal of the research was the concurrent enhancement of the impact strength and the heat resistance of recycled poly(ethylene terephthalate) (RPET). The morphology and the dynamic mechanical properties were examined at 0–5–10–15% ethylene-butyl-acrylate-glycidyl methacrylate (PTW) elastomer contents. The blends were crystallized for different time periods (0–20–40–60–180 s) at 150 °C and the morphology change during crystallization and its effect on impact resistance, stiffness, and thermal resistance were examined taking the three-phase model: crystalline fraction/mobile amorphous fraction/rigid amorphous fraction (CRF/MAF/RAF) into consideration. Based on DSC analyses it is proposed that before crystallization, the polymer chains covalently linked to PTW molecules contribute to the rigid amorphous phase (RAF). During thermal annealing, the relaxation of segments (which increases mobility) and ordering into crystals (which decreases mobility) have a complex effect and their resultant determines the ratio of the three phases and thereby also the macroscopic properties of the blends. After annealing the 15% PTW containing RPET blend at 150 °C for 180 s, a fivefold increase in notched impact resistance and a 50-fold increase in thermal resistance (expressed as E_{90} ' value) were achieved compared to the neat RPET reference.

Keywords Recycled PET · Thermal annealing · Impact modification · EBA-GMA

Introduction

In the last couple of years, the recycling of polymers became crucial [1, 2] as they realised that the current linear model is unsustainable. As an alternative, they promote the introduction of circular economy, in which the material and energy flow form a closed loop. One of its central ideas is maximizing the life cycle of products, as well as moderating consumption and utilizing renewable energy sources [3].

Plastics can be recycled mechanically and chemically. Mechanical recycling is the recollection, cleansing, grinding,

and reprocessing of waste produced during processing, scraps, and household waste. However, multiple processing in melt state is limited by the deteriorating mechanical and rheological properties [4]. During chemical recycling polymers are decomposed to valuable components, which can be used as feedstock in various chemical reactions.

The estimated annual production of poly(ethylene terephthalate) (PET) was 70 million tonnes in 2020 [5]. It is mainly applied in the form of fibres and packaging (films, bottles, trays) which are discarded at the end of their perpetual service time. However, the manufacturing of durable products for technical fields is hindered by the fragility and poor thermal resistance of amorphous PET. Many researchers have examined the toughening of PET, mainly by blending the polymer with elastomers [6–9]. The enhancement of heat resistance was also studied, generally by increasing the crystallinity of the PET [10–12].

Monti and others [7] examined the impact of glycidyl methacrylate (GMA) on the properties of fibre reinforced RPET composite. Despite the reduced molecular weight, the mechanical properties were favourable, especially the impact resistance. Latter can be explained by the reaction

✉ Katalin Bocz
boz.katalin@vbk.bme.hu

¹ Department of Organic Chemistry and Technology, Faculty of Chemical Technology and Biotechnology, Budapest University of Technology and Economics, Műegyetem Rkp. 3., Budapest 1111, Hungary

² Department of Innovative Vehicles and Materials, GAMF Faculty of Engineering and Computer Science, John Von Neumann University, H-Izsáki Str. 10., Kecskemét 6000, Hungary

between GMA and the –OH end-groups of PET chains which creates stable dispersed phase and lower interfacial tension.

Bocz et al. [6] studied the molecular weight of PET on impact resistance of PET/ethylene-butyl-acrylate-glycidyl methacrylate (EBA-GMA) blends. They recognized that the PET recyclates have more chain ends per unit volume and increased chain mobility and utilized this increased reactivity in reactive toughening. Noticeably upgrade in notched impact resistance was achieved at small elastomer content (10%), while similar results for PET is solely possible with higher ratios (20%) and with greater deterioration of stiffness. The short-chained RPET molecules provided better dispersion, as they can form more chemical bounds with the elastomer. The addition of a small amount of recycled PET to the original material was found to act as a toughening enhancer interphase (TEI).

As a continuation of the previous research [13] the effect of PET's moisture content on impact resistance was examined and it was found that certain amount of water promotes the hydrolytic degradation during processing resulting in the formation of short-chained PET fraction which is vital to effectively react with EBA-GMA. As a result, a sixfold improvement was reached in notched impact resistance, simply by omitting the conventional drying step of PET.

Chaudhari and Kale [8] studied the impact modification of waste PET by polyolefinic elastomer (POE) and poly(ethylene-co-acrylic acid) (EAA) as a compatibilizer. Due to EAA, not only the impact strength, but the tensile and flexural strength increased. The compatibilized blends had two melting peaks: the possible explanation is the presence of two types of PET crystals: PET interlocking POE at the interphase and crystals in the bulk.

Rahem et al. [14] studied the toughening of treated PET (trPET) with styrene-ethylene/butylene-styrene grafted with maleic anhydride (SEBS-g-MA). Before compounding, recycled PET was annealed at 150 °C for 5 h, which increased the crystallinity, and reduced the moisture capture capacity. The trPET blended with SEBS-g-MA not only showed better tensile, but higher impact resistance values, too.

Kelnar et al. [15] upgraded RPET with nonreactive rubber and clay, which acted as a compatibilizer and reinforcing agent. Clay caused a significant refinement of structure and the decrease of interparticle distance. However, the results were contradictory at times, which indicates the complexity of the system.

Oromiehie et al. [9] improved the properties of RPET by MA grafted polypropylene (PP-g-MA). It was found that RPET can be better for certain applications than original material because it crystallizes easier. PP-g-MA improved

the impact strength, but the tensile strength and modulus decreased.

Crystallinity and morphology strongly influence the properties of polymers. Crystallization can be mechanically or thermally induced [16]. The glass transition temperature (T_g) of semi-crystalline PET increases by 15–20 °C compared to the amorphous form. Besides, crystallized PET has elevated modulus, tensile strength, and chemical inertness, however, the impact resistance is worse.

Torres et al. [10] studied the thermal behaviour of original and recycled PET before and after processing. In recycled PET, the shorter chains are more mobile which promotes the crystallization. Besides that, contaminations and cyclic or linear oligomers can function as nucleating agents. Reduced intrinsic viscosity and lower molecular weight also help the faster arrangement of polymer chains.

Lu and Hay [11] studied the isotherm crystallization of PET from both glass and melt state. They concluded that the crystallization of PET consists of two consecutive steps: primary and secondary crystallization. The margin of the two processes is a critical degree of crystallinity, where the Avrami exponent suddenly decreases from 2.6 to 1.2.

Lin [12] also studied the izoterm crystallization of PET with DSC. From the change of Avrami exponent he assumed that secunder crystallization takes place and the reduction of the exponent was similar to what Lu and Hay reported: it decreased from 3 to 1.5. He noticed that crystallization slowed down with increasing molecular weight and by increasing the temperature in the 175–210 °C range.

Based on the newest researches, the morphology of PET can be described by a three-phase model [17]. The amorphous phase can be separated into two parts with distinct properties. The rigid amorphous fraction (RAF) is directly linked to the crystalline fraction (CRF) and its molecules are less mobile, compared to the mobile amorphous fraction (MAF). Besides the ratio of CRF, the amount and characteristics of RAF and MAF also have an impact on the products' mechanical properties.

Badia et al. [18] examined the properties of recycled PET by taking the three phase model into consideration. During processing the polymer in melt state, the chains break, which results in the reduction of molecular weight. The degradation was mainly induced by the rapture of MAF, and they also noticed the rearrangement of shorter PET chains into RAF. With increasing number of reprocessing cycles, crystallization started faster, but the ratio of CRF barely changed, while the lamellar thickness decreased.

The simultaneous improvement of impact resistance and crystallinity is rather challenging, as the increase of one property results in the reduction of the other. Billon and Meyer [19] studied the compounding of PET with core-shell elastomer particles. The crystallinity of the blends was controlled by the mould temperature. Two types of elastomer

systems were used and only one of them contained reactive epoxy groups on its surface. It is important, that while for the amorphous polymer both elastomer systems were effective, the impact resistance of semi-crystalline PET could only be efficiently increased by reactive toughening which provided proper adhesion and homogenous dispersion of the elastomer.

Loyens and Groeninckx [20] studied the impact strength of elastomer containing semi crystalline PET blends. The most efficient impact modifier was glycidyl methacrylate grafted on ethylene-propylene copolymer (EPR-g-GMAx). The morphology of the dispersed phase primarily determines the effectiveness of impact resistance enhancement. High E-GMAx content was unfavourable because of the crosslinking reactions, which caused irregular morphology. The distance of elastomer particles is also crucial, and the critical value was found to be 0.1 μm . It was seemingly independent of the functionality and quantity of GMA, as well as the type of compatibilizer agent.

Srithep et al. [21] characterized the properties of RPET blended with chain extender (CE), thermoplastic elastomer (TPE) and poly (butylene adipate-co-terephthalate) (PBAT). CE increased the molecular weight, viscosity, and mechanical properties. Crystallinity was further increased by annealing, which resulted in higher storage moduli, but lower strain-at-break.

Loyens and Groeninckx [22] examined the influence of the matrix polymer properties (molecular weight, crystalline ratio) and processing parameters on the impact strength of PET/elastomer systems. The blends were compression moulded with differing parameters to regulate their crystallinity. The dispersed phase was EPR and ethylene with glycidyl methacrylate (8 wt%), latter is a compatibilizer agent. Without compatibilizer, the structure was rough and heterogeneous, regardless the molecular weight. The high molecular weight matrix showed the strongest elastomer concentration dependence, which can be explained by the few chain-end groups. The low molecular weight matrix, even when the rubber particles were well dispersed, suffered brittle fracture, they were unable to stabilize the crack. Significant improvement can only be achieved at relatively high elastomer contents (20–30%).

The aim of the present research is to simultaneously improve the impact resistance and mechanical properties of PET with ethylene-butyl acrylate-glycidyl methacrylate terpolymer (PTW) as a reactive toughener and by post-crystallization. Based on previous research, the impact resistance of recycled PET can be upgraded more effectively by PTW than original PET [6], however, the incorporation of elastomer results in the reduction of tensile strength and stiffness. Our goal is to examine the

effect of post-crystallization on the mechanical properties of recycled PET blended with reactive elastomer. By enhancing the properties of recycled PET, its applicability may broaden, and the currently applied engineering thermoplastics might be replaced by a more sustainable option.

Applied Materials and Testing Methods

Applied Materials

Industrial quality recycled flakes (RPET) (Jász-Plasztik Kft., Hungary) were applied with an IV value of 0.56 ± 0.03 dl/g [6]. The recycle was produced from egg trays, which were sheet extruded and thermoformed then grinded. The additive was Elvaloy PTW (DuPont, USA) which consists of ethylene (66.75 wt%), butyl-acrylate (28.00 wt%) and glycidyl methacrylate (5.25 wt%). Its melt flow rate is 12 g/10 min (measured at 190 °C with 2.16 kg load), the peak temperature of melting is 72 °C and the T_g is – 55 °C [23].

From the grinded tray material (RPET) 4 compositions were made with different PTW contents of 0, 5, 10 and 15 wt%, respectively.

Sample Preparation

The blends were prepared on an LTE 26–48 (Labtech Scientific, Thailand) extruder with twin-screw. Prior to extrusion, the PET underwent a 3 h long drying process at 160 °C. The zone temperatures were between 250 and 260 °C during processing. The pressure inside the extruder barrel when it was operated at 90 rpm screw rotation speed is summarized in Table 1. The melt pressure increased quasi linearly with the PTW content.

The regranulate was dried for 4 h at 150 °C, then plaques with 2 mm thickness were produced on a 50MetII injection moulding apparatus (Mitsubishi, Japan). The zone temperatures were 255–245 °C. The temperature of the mould was 40 °C and a 50 MPa holding pressure was applied for 4 s.

Table 1 Pressure during extrusion

RPET (wt%)	PTW (wt%)	Pressure (bar)
100	0	43
95	5	47
90	10	49
85	15	56

The thermal annealing of the injection moulded plaques was done at 150 °C in a preheated Memmert Une 200 drier and the sample was placed between two aluminium moulds for 20–40–60–180 s.

Test Methods

On the quasi amorphous and crystallized samples DSC measurements were done in inert medium. First, the samples were heated from 20 to 320 °C at 20 °C/min, then kept at 320 °C for 5 min, then cooled to 20 °C with the same rate and after 5 min they were heated in the same way as during the first heating cycle. The crystalline ratio achieved by thermal annealing was calculated from the crystalline melting peak of the DSC curve during the first heating scan. The results were corrected by the crystalline fraction which was detected during the heating and the PTW content was also considered. The following equation was used for the calculations:

$$CRF = \frac{\Delta h_m - \Delta h_{cc}}{\Delta h_m^0 \cdot (1 - w_{PTW})} \times 100\% \quad (1)$$

where CRF is the crystalline fraction (%), Δh_m is the weight specific melting enthalpy of the sample (J/g), Δh_{cc} is the weight specific cold crystallization enthalpy (J/g), Δh_m^0 is the weight specific melting enthalpy of the 100% crystallized PET (140 J/g), w_{PTW} is the weight fraction of PTW (-) [18].

Besides the crystalline fraction, the amount of mobile amorphous phase (MAF) was also determined from the specific heat change registered at the glass transition, with the help of the following equation:

$$MAF = \frac{\Delta c_p}{\Delta c_p^0 \cdot (1 - w_{PTW})} \times 100\% \quad (2)$$

where MAF is the amount of mobile amorphous phase (%), Δc_p is the specific heat change of the sample during glass transition (J/(g·K)), and Δc_p^0 is the specific heat change of 100% amorphous PET during glass transition (0.405 J/(g·K)). The relative size of the rigid amorphous phase (RAF) (%) can be calculated from CRF and MAF with the following equation [18]:

$$RAF = 100 - MAF - CRF \quad (3)$$

Specimens with 10 mm width were crafted from the moulded parts and then were polished until 3 µm surface roughness was reached. The specimens were notched and hit by a 5.5 J Izod pendulum with 0.02 J pendulum energy. The results provide information on the effect of PTW on impact resistance.

During the DMA measurements, dynamic tensile tests were carried out on the test specimens with 10 Hz frequency,

the temperature was increased from 10 to 140 °C with an increment of 3 °C/minute. The size of the specimen was 30 × 8 × 2 mm. The clamping jaws were 20.08 mm apart. The improvement in stiffness and heat resistance achieved by thermal annealing can be studied by this method.

The Izod test specimens containing PTW were bedded in acrylic resin and polished, then dissolved in toluene at room temperature for 2 h to remove the PTW phase. The samples were dried overnight in a vacuum drier at 60 °C and 90 mbar to remove the chemical residues from the surface. The polished resins were coated with gold and examined by Zeiss EVO MA10 scanning electron microscope (SEM) with secondary and backscattered electron detector. The accelerating voltage was 16 kV, the spot size was 472 and the working distance was 10.5–12 mm. To determine the particle size distributions, the SEM micrographs have been analysed with AxioVision SE64 Rel, 4.9.1 software. 700–1000 particles on each SEM image have been measured manually.

Results and Discussion

Change of Mechanical Performance During Thermal Annealing

The objective of the current study was to achieve concurrent advancement of impact strength, stiffness, and thermal resistance in RPET based blends. One of the obstacles regarding the application of semi-crystalline PET -rigidity- was improved by PTW, which based on previous research [6], is an effective toughening agent.

Figure 1 illustrates the change of impact resistance as the function of crystallization time at 150 °C. The impact behaviour of uncrystallized RPET samples was already tough at

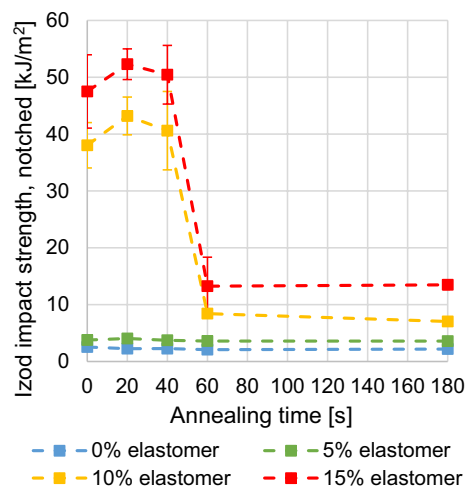


Fig. 1 Impact strength versus annealing time

only 10% elastomer content (similar results with original PET can be achieved by the addition of 20–25% elastomer [6]). At short crystallization times (20 and 40 s) the impact resistance even slightly increased compared to the amorphous samples. After 60 s, the previously tough samples showed a more brittle behaviour and the impact strength values reduced to their fraction, which did not decrease further by longer thermal annealing (180 s).

The impact resistance of samples with 15% PTW decreased from 48 kJ/m² to 13 kJ/m² over the course of 180 s crystallization. When the impact strength values measured after 180 s of thermal annealing are compared, the changes with the PTW contents are less drastic compared to the differences observed between the uncrystallized blends. The improvement of impact strength after 180 s annealing, however, can be called successful at higher (10–15%) PTW contents, as the values are 5–6-times higher than that of the neat polymer.

The addition of elastomer usually decreases stiffness, which can be characterized by room temperature storage modulus (E_{23}') [24]. By crystallizing the samples, the goal is to simultaneously enhance stiffness and thermal stability. Latter was expressed by the storage modulus at 90 °C (E_{90}'). E_{23}' , E_{90}' and the glass transition temperature were determined from DMA measurements. E_{23}' values increased until 60 s thermal annealing, after that the results were quasi constant (Fig. 2a). The highest E_{23}' value of 2190 MPa was measured for the 100% RPET sample at 60 s. Increasing PTW contents resulted in the decrease of E_{23}' .

Analysing the E_{90}' values, the small moduli of the uncrystallized samples rapidly increase between 40 and 60 s annealing time, which is followed by a slight improvement between 60 and 180 s (Fig. 2b). The increase of E_{90}' at 5% PTW content begins a bit earlier, at around 20–40 s. The

best heat resistance results were achieved after 180 s, when the moduli increased by 370–580 MPa compared to the uncrystallized specimens.

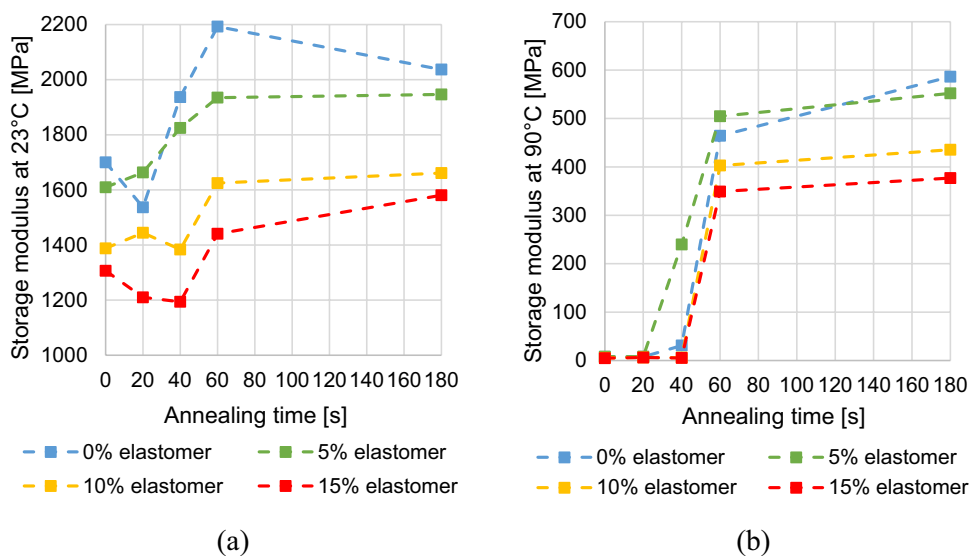
As one of the principled difficulties regarding PET is its poor heat resistance, the enhancement achieved at higher temperature (90 °C) is key. It reflects that with well-designed composition and structure, PET can become raw material for durable technical goods. Also, 90 °C is above the glass transition temperature (T_g), therefore the amorphous phase is already in rubbery state. The crystalline fraction can reinforce the rubbery segments more successfully, than the more rigid chains in glass state [25].

It is important to note, that the improvement in storage moduli at 23 °C achieved by annealing (Fig. 2a) is overshadowed by the deterioration of impact strength (Fig. 1). However, even after longer annealing times (60–180 s), the impact resistance is still significantly higher than that of neat RPET.

Change of Morphology During Crystallization

The distribution of PTW particles was examined based on SEM images, which were taken after the embedding resin was polished and the elastomer was selectively dissolved in toluene (Fig. 3). The phase structure was studied before annealing and after 180 s crystallization, as PTW enters the melt phase at the crystallization temperature, which can affect the dispersed particles. Figure 4 compares the particle size distribution of the elastomer phase in the PET/PTW blends, determined by measuring 700–1000 particles on each SEM image, before and after crystallization (150 °C, 180 s). As it is presented in Table 2, at a given PTW content, very similar median values were obtained, although the

Fig. 2 a E_{23}' and E_{90}' b as the function of annealing time



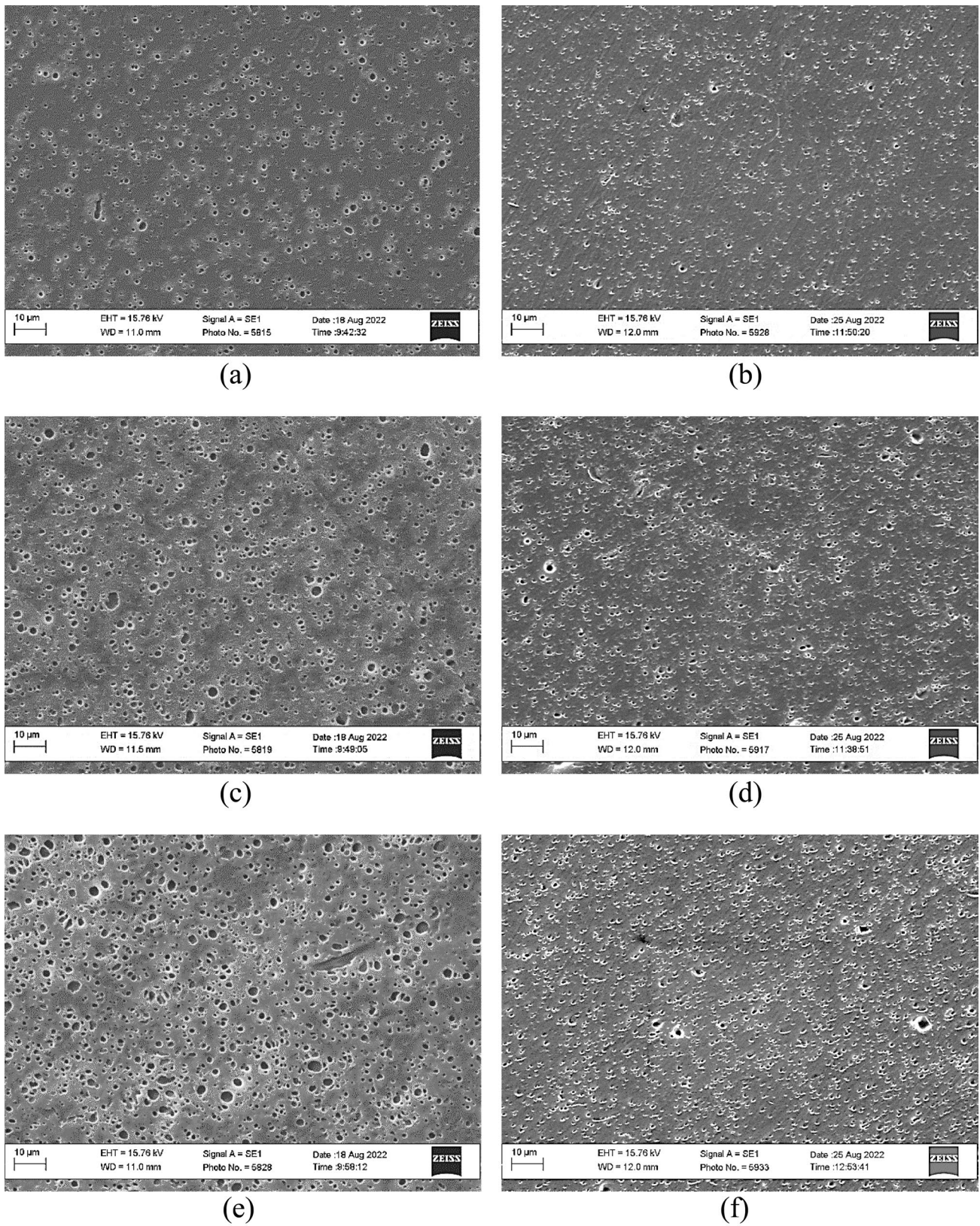


Fig. 3 SEM images of samples with 5-10-15% elastomer content at 2000 \times magnification: **a–c–e** before crystallization and **b–d–f** after crystallization

Fig. 4 Relative frequency diagrams of the PTW particles in PET/PTW blends with **a** 5%, **b** 10% and **c** 15% elastomer content

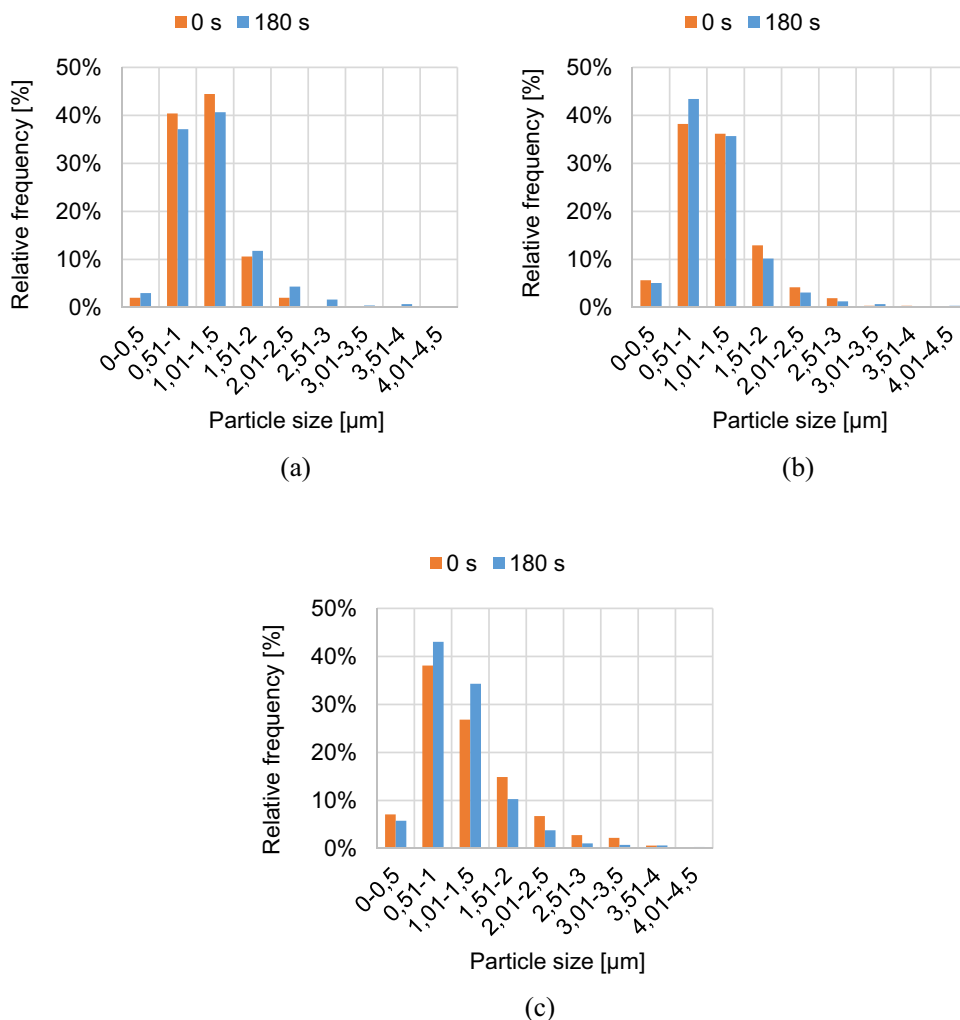


Table 2 The number-weighted mean and median diameter of the PTW particles in PET/PTW blends before and after annealing at 150 °C for 180 s

Elastomer content [%]	0 s			180 s		
	mean [μm]	median [μm]	SD [μm]	mean [μm]	median [μm]	SD [μm]
5	1.13	1.04	0.45	1.20	1.06	0.56
10	1.16	1.06	0.56	1.12	1.03	0.55
15	1.26	1.06	0.75	1.12	1.03	0.57

standard deviations (SD) are quite large, i.e. the distributions are quite wide. Since SEM micrographs did not show significant difference between the morphology of the crystallized and uncrystallized samples, it was concluded that the change of mechanical properties is not due to the change of elastomer dispersion during crystallization.

The Change of Crystalline Fraction and Glass Transition Temperature During Crystallization

The crystalline structure of PET matrix was investigated with the aim of finding a relation with the observed impact

resistance changes. In Fig. 5 the crystalline fraction ratios determined from DSC curves are presented as the function of crystallization time. The crystallinity rapidly changed from 8 to 10% to 23–26% between 40 and 60 s, but above that, only a slight change can be noticed. The sample with 5% PTW content showed a bit different behaviour: the crystalline fraction already increased significantly between 20 and 40 s.

Figure 4 indicates that the influence of PTW on crystallization is smaller compared to the impact of annealing time,

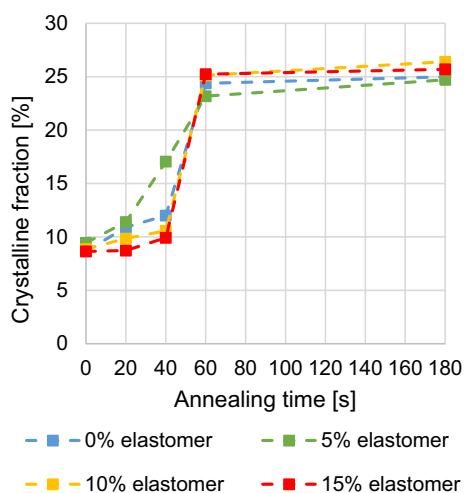


Fig. 5 The change of crystalline fraction with annealing time

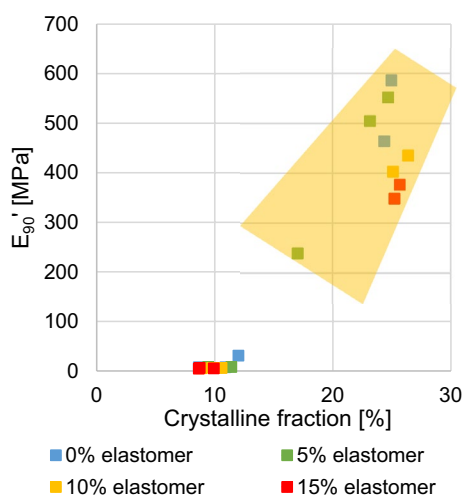


Fig. 6 E'_{90} as the function of crystalline fraction

as the character of ramp-up and the maximal crystalline ratio only slightly change with increasing PTW content.

The change of E'_{90} with annealing time (Fig. 2b) shows a similar trend to the change of crystallinity (Fig. 5): both increase until 60 s, but further annealing does not result in further growth. Impact resistance decreases with annealing time as Fig. 1 indicates it. This suggests that impact resistance is determined by CRF, as well. However, the trend is not the total opposite of how crystallinity and E'_{90} changed. It can be highlighted, that between 0 and 40 s, the impact resistance slightly grows, then drastically reduces, while crystallinity already starts to increase after 20 s of annealing.

The correlation between E'_{90} and the ratio of crystalline fraction is presented in Fig. 6. It can be observed that a

critical, minimum crystalline ratio must be exceeded (appr. 18%) to achieve significant improvement in E'_{90} values.

As it is presented in Fig. 7a, post-crystallization shifts the glass transition temperature towards higher values, which means that the polymer can be applied at higher operating temperatures without the significant deterioration of stiffness, which is a great potential to broaden the applicability of low thermal-resistance PET. PTW content does not noticeably influence the values of T_g , even though some of the molecules are covalently linked to the PTW particles [6, 13, 26]. This is due to the melting of PTW at 70 °C, which no longer put a compulsion on the PET chains. Huang et al. [27] annealed PET samples at 100 °C for 0–80 min and while the ratio of crystalline fraction greatly increased (after 80 min it reached 21.5%) the glass transition temperature was only 76.5 °C. In contrast, after 180 s at 150 °C, the T_g of our samples was above 85 °C with similar crystallinity ratios. The step-like growth of E'_{90} (Fig. 7b) is also associated with the observed increase in glass transition temperature.

Effect of PTW Content on Crystallization Properties

Figure 8a illustrates the change of peak temperature of crystallization (T_c) with elastomer ratio. The T_c closely linearly decreased with rising PTW content. Figure 8b shows the crystalline fraction, which was formed during cooling, after the thermal life was erased. Interestingly, the sample with 5% PTW could achieve the highest crystalline ratio, but the difference was not significant, even though Fig. 8a does not indicate nucleating effect at that specific composition. Based on the research carried out by Zhang et al. [28] it is assumed that the formation of PET-EBA-GMA copolymer increases the intermolecular interaction. On the one hand, the elastomer particles hinder the mobility of the macromolecules and reduces T_c (Fig. 8a). On the other hand, the reaction of PET and PTW induce the augmentation of the polymer on the surface of elastomer particles, according to Ronkay and others [13], and thus, at 5% PTW content the orderly arrangement of PET chains eases the crystallization of PET (Fig. 8b).

The Effect of Crystallite Size and Ratio of Rigid/ Mobile Amorphous Phase on Properties

The peak temperature of crystalline melting – according to the Gibbs-Thompson equation – is in connection with the surface/volume ratio of crystalline formations, which is primarily determined by the lamellar size [6]. The peak temperature of crystalline melting is presented as the function of thermal annealing time in Fig. 9a. It can be observed that the lamellar thickness only increases in the case of pure RPET at the beginning of the annealing. However, as it is

Fig. 7 **a** Glass transition temperature as the function of annealing time and **b** E'_{90} as the function of glass transition temperature

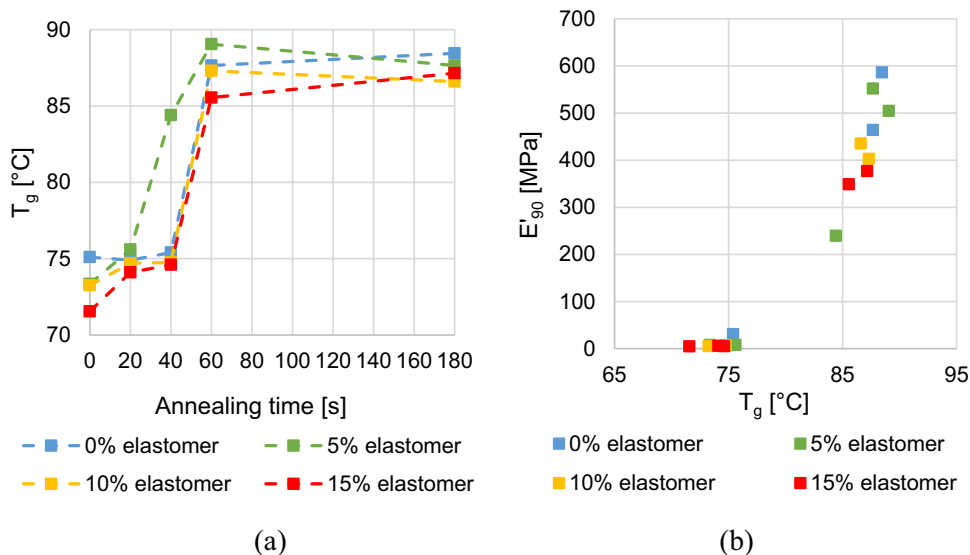
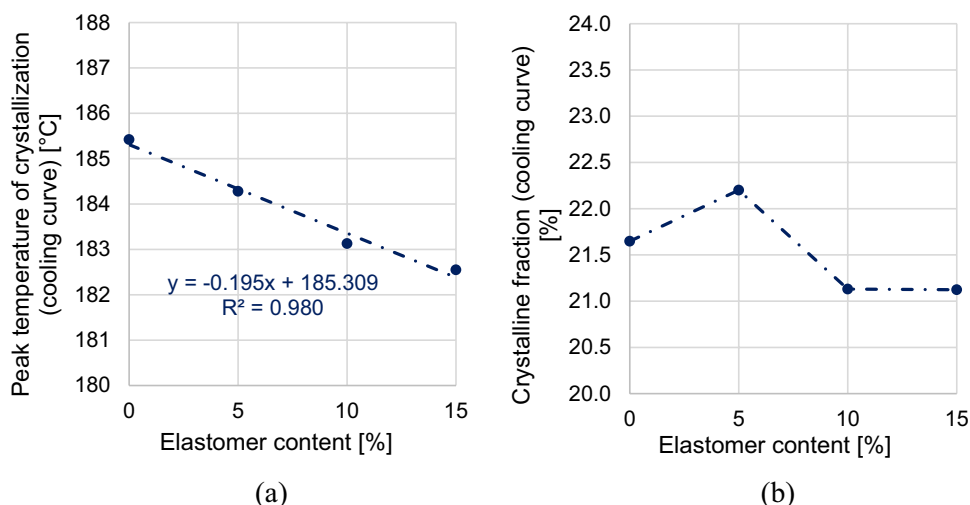


Fig. 8 **a** Peak temperature of crystallization as the function of PTW content and **b** crystalline fraction as the function of elastomer ratio



presented in Fig. 9b, during the first heating, cold crystallization occurred at certain samples.

According to the three-phase model [17] the molecules in the rigid amorphous phase (RAF) which is located right next to the crystalline phase are less agile, while the chains in the mobile amorphous phase (MAF) can move more freely. Figure 10 illustrates the change of MAF and RAF as the function of crystallization time. A clear increasing or decreasing trend cannot be noticed with increasing annealing time. This phenomenon and the fact that the ratio of RAF increases with the PTW content for the uncrystallized samples (Fig. 10a) suggest that not only the molecular chains around the crystalline fraction, but also the ones being covalently linked to PTW particles are immobile, and thus contribute to the rigid amorphous phase. The ratio of MAF (Fig. 10b) increases at shorter annealing times, then after 40 s it starts to decrease. It is proposed that at the beginning

of thermal annealing the segments relax on the interface, and the chains in constrain become more mobile, which results in the increase of MAF/RAF ratio. The melting of PTW also contributes to the relaxation of polymer chains. After longer time periods, crystallization becomes the dominant process, which constrains the chains again, thus the amount of RAF grows.

The ratio of the three phases as the function of PTW content is presented in Fig. 11. Figure 11a indicates that before crystallization with increasing elastomer content the ratio of crystalline phase remains quasi constant, while the amount of MAF decreases and RAF grows in the examined range of elastomer ratio. After 180 s annealing (Fig. 11b), the ratio of CRF increases to 24–26% regardless the elastomer content. The ratio of RAF/MAF also increases due to the annealing, however, the ratio of RAF decreases with the PTW content.

Fig. 9 **a** Peak temperature of crystalline melting and **b** the peak temperature of cold crystallization as the function of annealing time

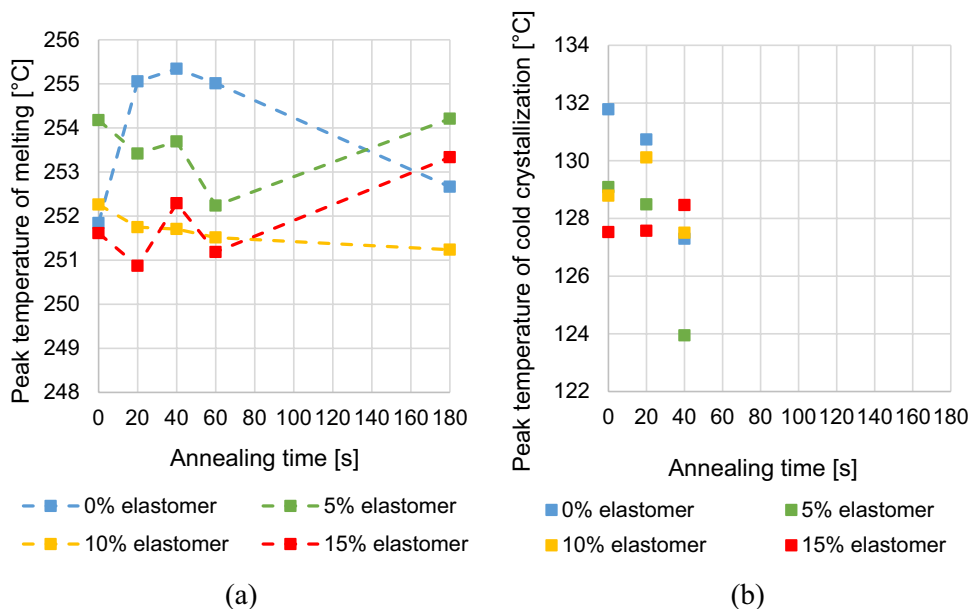


Fig. 10 **a** RAF and **b** MAF ratios as the function of annealing time

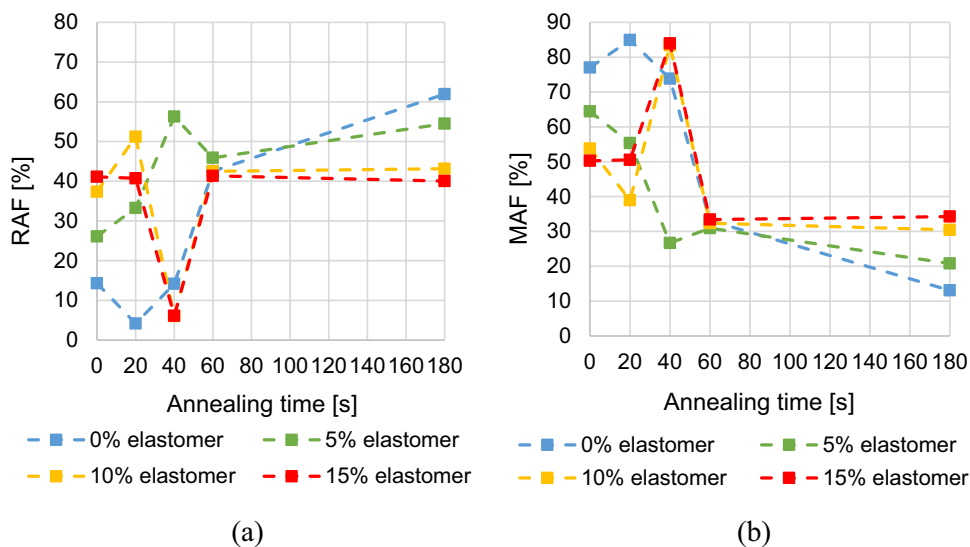


Fig. 11 CRF, MAF and RAF as the function of PTW **a** in the case of uncrystallized samples and **b** after crystallized for 180 s

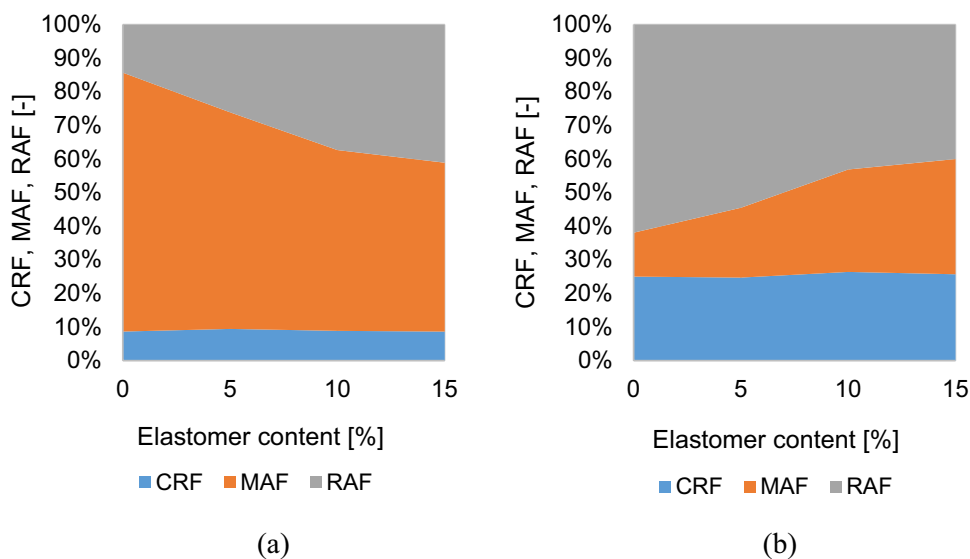


Fig. 12 **a** RAF and **b** MAF as the function of the crystalline fraction (every annealing time presented)

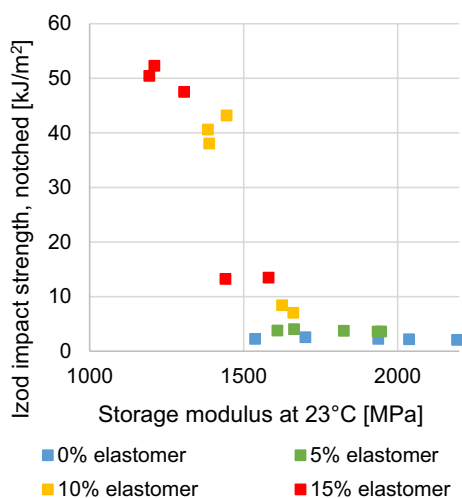
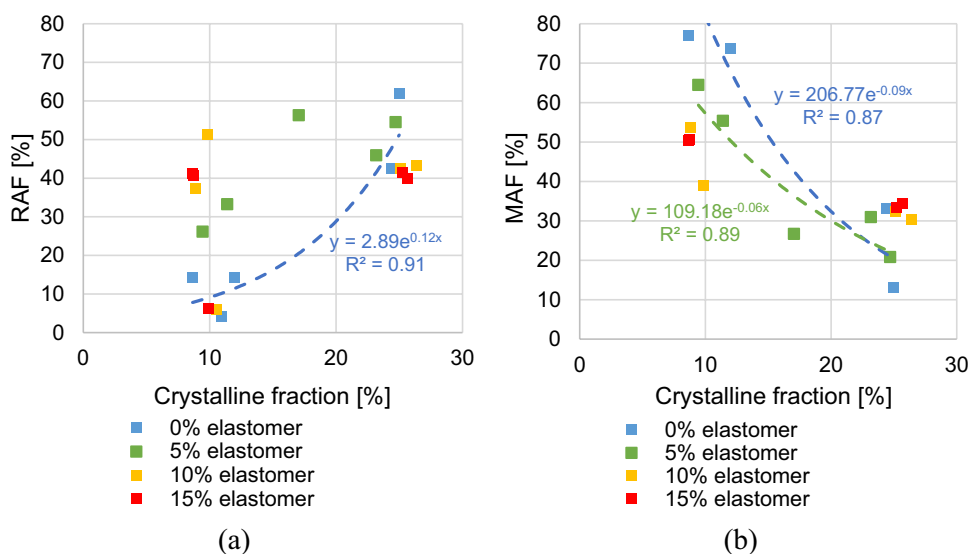


Fig. 13 E_{23}^* as the function of impact resistance

According to the literature [12], RAF can mainly be found around the crystalline phase, hence there should be a correlation between CRF and RAF. Based on our DSC analysis (Fig. 12), this theory appropriately describes the behaviour of pure RPET, where besides CRF only the amount of internal stress influences the RAF, and an exponential relationship can be observed. However, no clear correlation was detected between CRF and RAF for the PET-PTW blends. This observation also confirms the assumption that RAF is not only determined by the ratio of crystallinity, but the PTW content also influences it.

The relation between the impact resistance and stiffness (E_{23}^*) is presented in Fig. 13. At higher PTW contents (10–15%) the impact strength decreases exponentially with E_{23}^* . This is due to reaching a critical crystalline ratio

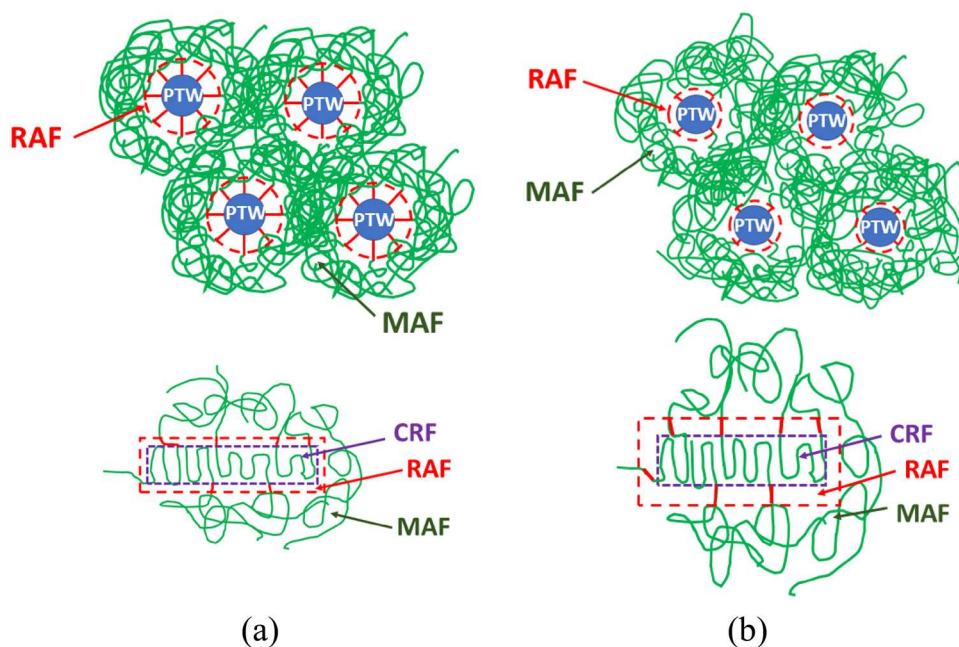
(18–20%), which also results in the significant increase of glass transition temperature.

Another important result of our research comes from the DSC measurements analysed by the three-phase model. It was found that with increasing PTW content, the ratio of rigid and mobile amorphous phase (RAF/MAF) rises. Based on this, it is assumed, that some segments of PET chains attached to the elastomer particles are immobile. The proposed model is presented in Fig. 14. Before crystallization, the polymer chains covalently linked to PTW molecules contribute to the RAF. During annealing, first the compulsion of PTW molecules disappear due to the melting of the elastomer, then, the PET segments are restricted again as they crystallize, and the rigid amorphous phase thickens around the crystallites. No reference was found in the literature regarding such description of phase structure in polymer blends. It is also important that the amount of RAF and MAF do not change evenly during crystallization: the relaxation of segments (which increases mobility) and crystallization (which decreases mobility) have a complex effect and their resultant determines the ratio of the three phases and thereby also the macroscopic properties of the blends.

Conclusions

In this study, it was explored how post-crystallization influences the morphology and mechanical performance of RPET/PTW blends. It was found that after 180 s annealing at 150 °C, the impact resistance of the PET/PTW blends significantly decreases compared to the uncrystallized samples and the correlation between the elastomer content and impact strength changes from rapid growth to slight increase with increasing PTW ratio. It was evinced based

Fig. 14 morphology of RPET-PTW systems in accordance with the three-phase model **a** before crystallization; and **b** after crystallization



on SEM images that the size of PTW particles does not change during crystallization. Stiffness and thermal resistance were found to be primarily determined by the ratio of crystalline fraction of the blends. Based on DSC results, the effect of PTW is less considerable on the ratio of crystalline phase than the impact of annealing time. Before annealing, E_{23}' decreases with increasing PTW ratio. As a function of crystallization time E_{23}' is increasing until 60 s, after that the values barely change. Significant upgrade of thermal resistance only occurs above a critical (approx. 18%) CRF. This phenomenon was also observed in the case of glass transition temperature, where a 10 °C increase was noticed.

The indirect exploitation of the present research, which is of practical relevance, is that by blending recycled PET with relatively low amount of PTW, high impact resistance and stiffness, as well as improved thermal resistance, can be reached. The notched impact resistance of toughened (15% PTW) and crystallized RPET blend is about 5-times higher than that of uncrystallized 100% RPET, while in the thermal resistance values (E_{90}') a 50-fold increase was achieved. By this approach, not only the production costs of engineering plastics can be cut, but the requirements of circular economy can be met by applying recycled material.

Supplementary Information The online version contains supplementary material available at <https://doi.org/10.1007/s10924-023-02945-4>.

Author Contributions Conceptualisation, FR and KB; methodology, SE and FR; investigation, SE; evaluation SE, FR and KB; visualisation, SE; writing, SE, FR and KB. All authors have read and agreed to the published version of the manuscript.

Funding Open access funding provided by Budapest University of Technology and Economics. The project was funded by the National Research, Development and Innovation Fund of Hungary in the frame of the 2019–1.3.1-KK-2019–00004 and GINOP_PLUSZ-2.1.1-21-2022-00041 projects. The research was funded by the Hungarian Scientific Research Fund, Grant Number FK128352. The research was funded by the Sustainable Development and Technologies National Programme of the Hungarian Academy of Sciences (FFT NP FTA).

Declarations

Competing interests The authors declare no competing interests.

Open Access This article is licensed under a Creative Commons Attribution 4.0 International License, which permits use, sharing, adaptation, distribution and reproduction in any medium or format, as long as you give appropriate credit to the original author(s) and the source, provide a link to the Creative Commons licence, and indicate if changes were made. The images or other third party material in this article are included in the article's Creative Commons licence, unless indicated otherwise in a credit line to the material. If material is not included in the article's Creative Commons licence and your intended use is not permitted by statutory regulation or exceeds the permitted use, you will need to obtain permission directly from the copyright holder. To view a copy of this licence, visit <http://creativecommons.org/licenses/by/4.0/>.

References

- Zhou H et al (2022) Recycling end-of-life WPC products into ultra-high-filled, high-performance wood fiber/polyethylene composites: a sustainable strategy for clean and cyclic processing in the WPC industry. *J Mater Res Technol.* <https://doi.org/10.1016/j.jmrt.2022.02.091>
- Techawinyutham L, Tengsuthiwat J, Srisuk R, Techawinyutham W, Mavinkere Rangappa S, Siengchin S (2021) Recycled LDPE/PETG blends and HDPE/PETG blends: mechanical, thermal, and

- rheological properties. *J Res Technol Mater*. <https://doi.org/10.1016/j.jmrt.2021.09.052>
3. Korhonen J, Honkasalo A, Seppälä J (2018) Circular economy: the concept and its limitations. *Ecol Econ*. <https://doi.org/10.1016/j.ecolecon.2017.06.041>
 4. Valerio O, Muthuraj R, Codou A (2020) Strategies for polymer to polymer recycling from waste: current trends and opportunities for improving the circular economy of polymers in South America. *Curr Opin Green Sustain Chem*. <https://doi.org/10.1016/j.cogsc.2020.100381>
 5. Dai L et al (2021) Enhancing PET hydrolytic enzyme activity by fusion of the cellulose-binding domain of cellobiohydrolase I from *Trichoderma reesei*. *J Biotechnol*. <https://doi.org/10.1016/j.jbiotec.2021.05.006>
 6. Bocz K, Ronkay F, Decsov KE, Molnár B, Marosi G (2021) Application of low-grade recyclate to enhance reactive toughening of poly(ethylene terephthalate). *Polym Degrad Stab*. <https://doi.org/10.1016/j.polymdegradstab.2021.109505>
 7. Monti M, Scrivani MT, Kociolek I, Larsen ÅG, Olafsen K, Lambertini V (2021) Enhanced impact strength of recycled PET/glass fiber composites. *Polymers (Basel)*. <https://doi.org/10.3390/polym13091471>
 8. Chaudhari KP, Kale DD (2003) Impact modification of waste PET by polyolefinic elastomer. *Polym Int*. <https://doi.org/10.1002/pi.1071>
 9. Oromiehie A, Mamizadeh A (2004) Recycling PET beverage bottles and improving properties. *Polym Int*. <https://doi.org/10.1002/pi.1389>
 10. Torres N, Robin JJ, Boutevin B (2000) Study of thermal and mechanical properties of virgin and recycled poly(ethylene terephthalate) before and after injection molding. *Eur Polym J*. [https://doi.org/10.1016/S0014-3057\(99\)00301-8](https://doi.org/10.1016/S0014-3057(99)00301-8)
 11. Lu XF, Hay JN (2001) Isothermal crystallization kinetics and melting behaviour of poly(ethylene terephthalate). *Polymer (Guildf)*. [https://doi.org/10.1016/S0032-3861\(01\)00502-X](https://doi.org/10.1016/S0032-3861(01)00502-X)
 12. Lin CC (1983) The rate of crystallization of poly(ethylene terephthalate) by differential scanning calorimetry. *Polym Eng Sci*. <https://doi.org/10.1002/pen.760230302>
 13. Ronkay F, Molnár B, Szabó E, Marosi G, Bocz K (2022) Water boosts reactive toughening of PET. *Polym Degrad Stab*. <https://doi.org/10.1016/j.polymdegradstab.2022.110052>
 14. Zahir Rahem A, Douibi A, Lallam C, Delaite, Guessoum M (2019) Synergistic Combination of Crystallization and Addition of a Toughening Agent to Promote Recycled Poly(ethylene terephthalate) Performances. *Polym Sci - Ser A*. <https://doi.org/10.1134/S0965545X19050158>
 15. Kelnar I, Sukhanov V, Rotrekl J, Kaprálková L (2010) Toughening of recycled poly(ethylene terephthalate) with clay-compatible rubber phase. *J Appl Polym Sci*. <https://doi.org/10.1002/app.31905>
 16. Demirel B, Yaraş A, Elçiçek H (2011) Crystallization behavior of PET materials. *BAÜ Fen Bil Enst Derg Cilt* 13(1):26–35
 17. Rastogi R, Vellinca WP, Rastogi S, Schick C, Meijer HEH (2004) The three-phase structure and mechanical properties of poly(ethylene terephthalate). *J Polym Sci Part B Polym Phys*. <https://doi.org/10.1002/polb.20096>
 18. Badia JD, Strömberg E, Karlsson S, Ribes-Greus A (2012) The role of crystalline, mobile amorphous and rigid amorphous fractions in the performance of recycled poly(ethylene terephthalate) (PET). *Polym Degrad Stab*. <https://doi.org/10.1016/j.polymdegradstab.2011.10.008>
 19. Billon N, Meyer JP (2003) “Experimental study of rubber-toughening of pet”, in European Structural Integrity Society. Elsevier, Amsterdam
 20. Loyens W, Groeninckx G (2002) Ultimate mechanical properties of rubber toughened semicrystalline PET at room temperature. *Polymer (Guildf)*. [https://doi.org/10.1016/S0032-3861\(02\)00472-X](https://doi.org/10.1016/S0032-3861(02)00472-X)
 21. Srihthep Y et al (2011) Processing and characterization of recycled poly(ethylene terephthalate) blends with chain extenders, thermoplastic elastomer, and/or poly(butylene adipate-co-terephthalate). *Polym Eng Sci*. <https://doi.org/10.1002/pen.21916>
 22. Loyens W, Groeninckx G (2002) Rubber toughened semicrystalline PET: Influence of the matrix properties and test temperature. *Polymer (Guildf)*. [https://doi.org/10.1016/S0032-3861\(02\)00743-7](https://doi.org/10.1016/S0032-3861(02)00743-7)
 23. Yuryev Y, Mohanty AK, Misra M (2016) Hydrolytic stability of polycarbonate/poly(lactic acid) blends and its evaluation via poly(lactic acid) median melting point depression. *Polym Degrad Stab*. <https://doi.org/10.1016/j.polymdegradstab.2016.10.011>
 24. López-Suevos F, Eyholzer C, Bordeanu N, Richter K (2010) DMA analysis and wood bonding of PVAc latex reinforced with cellulose nanofibrils. *Cellulose*. <https://doi.org/10.1007/s10570-010-9396-8>
 25. Shieh YT, Lin YS, Twu YK, Tsai HB, Lin RH (2010) Effect of crystallinity on enthalpy recovery peaks and cold-crystallization peaks in PET via TMDSC and DMA studies. *J Appl Polym Sci*. <https://doi.org/10.1002/app.31570>
 26. You X, Snowdon MR, Misra M, Mohanty AK (2018) Biobased Poly(ethylene terephthalate)/Poly(lactic acid) blends tailored with epoxide compatibilizers. *ACS Omega* 3(9):11759–11769. <https://doi.org/10.1021/acsomega.8b01353>
 27. Huang JM, Chu PP, Chang FC (2000) Conformational changes and molecular motion of poly(ethylene terephthalate) annealed above glass transition temperature. *Polymer (Guildf)*. [https://doi.org/10.1016/S0032-3861\(99\)00329-8](https://doi.org/10.1016/S0032-3861(99)00329-8)
 28. Zhang Y, Zhang H, Ni L, Zhou Q, Guo W, Wu C (2010) Crystallization and mechanical properties of recycled poly(ethylene terephthalate) toughened by styrene-ethylene/butylenes-styrene elastomer. *J Polym Environ*. <https://doi.org/10.1007/s10924-010-0223-y>

Publisher's Note Springer Nature remains neutral with regard to jurisdictional claims in published maps and institutional affiliations.